applied sciences

MDPI

Technical Note

An Analytical Solution to Two-Region Flow Induced by Constant-Head Pumping in an Unconfined Aquifer

Yijie Zong and Liang Xiao *

College of Civil Engineering and Architecture, Guangxi University, Nanning 530004, China
* Correspondence: gxuxl@gxu.edu.cn

Abstract: This paper proposes an analytical solution to the problem of two-region flow induced by constant-head pumping tests in an unconfined aquifer based on the Dupuit assumption. The two-region flow includes a finite non-Darcian pattern near the pumping well and a semi-finite Darcian pattern in the rest region. By Izbash's equation, the solution to the two-region flow is derived using the Boltzmann method. The reliability of the proposed solution is investigated through comparisons with the numerical solution by COMSOL Multiphysics and the hydraulic head−time data from the pumping test in Wisconsin. The influences of the finite non-Darcian flow pattern on the hydraulic head and pumping rate are also discussed. The results demonstrate that a greater degree of non-Darcian turbulence can effectively increase the pumping flow rate, although such influence can be reduced over time. A method for determining the range of the non-Darcian region has been developed and validated by the specific discharge and Reynolds number.

Keywords: constant-head test; unconfined aquifer; two-region flow; non-Darcian effect; analytical solution

Citation: Zong, Y.; Xiao, L. An Analytical Solution to Two-Region Flow Induced by Constant-Head Pumping in an Unconfined Aquifer. *Appl. Sci.* **2022**, *12*, 11493. https://doi.org/10.3390/app122211493

Academic Editors: Ladislav Dzurenda, Richard Lenhard and Jozef Jandačka

Received: 3 September 2022
Accepted: 10 November 2022
Published: 12 November 2022

1. Introduction

Constant-head test is a special pumping test that maintains a fixed drawdown in a pumping well [1,2]. It is typically conducted in formations of low hydraulic conductivity where it would be difficult to sustain a constant rate of pumping [3–5]. The constant-head test is valuable for the determination of hydraulic parameters or for solving environmental damage in landfills [3]. Since 1950, the mechanics of such pumping flow induced by the constant-head test have been especially studied by hydrogeologists. In 1950, Jacob proposed the first analytical solution for the investigation of Darcian flow behavior during the constant-head pumping test [6]. After then, substantial effective work has been done on numerical and analytical modeling of the constant-head pumping flow [7–10].

In general, the pumping-induced flow is obeyed by Darcian law with a linear flow assumption [11–13]. However, many scholars have to note that the specific discharge can be nonlinearly related to the hydraulic gradient when the gradient is sufficiently large or small [14–16]. Such nonlinear pumping flow is defined as non-Darcian flow [12], which is commonly depicted by Izbash's equation or Forchheimer's equation. The choice between the two equations depends on the field conditions [14,15]. By the two methods, the issues of the non-Darcian effect on flow behaviors induced by constant-head pumping have been studied via in situ tests and numerical modeling in the last decade [8,16]. For example, Quinn et al. [16] carried out a constant-head slug test in fractured dolostone and sandstone near the city of Guelph, Ontario, Canada, and suggested that using a linear type of Darcian flow to fit experimental data could produce a large error. Specifically, the hydraulic gradient−time curve of the pumping data was expressed by an obvious exponential relationship, and the deviation of its comparison with the Darcian solution was found to be increased with time. Dan et al. [8] evaluated the parameters of unbound graded aggregates based on the drawdown data of constant-head tests and found that the non-Darcian flow was widespread even under a low hydraulic gradient. Liu et al. [10]

conducted a constant-head test in a saturated clay aquifer using an improved permeability test device and proposed a numerical solution using the finite difference method to simulate the flow induced by constant-head pumping. The results indicated an obvious non-Darcian characteristic of the pumping-induced flow. These studies have also noticed that neglecting the non-Darcian effect can introduce severe errors in pumping-flow simulation and aquifer parameter determination. Thus far, few studies have been conducted to analytically investigate such non-Darcian flows in response to constant-head pumping. To our knowledge, Li et al. [17] proposed the first analytical solution to the non-Darcian flow induced by the constant-head test using an aquifer injection well. Their model with time-dependent conductivity was developed using the Laplace transform based on Izbash's equation with a constant non-Darcian coefficient in the entire confined aquifer.

Based on the careful literature review, the authors noted that the existing solutions for the constant-head test are generally proposed based on the assumption that the pumped aquifer is confined. However, many pumping wells are located in unconfined aquifers worldwide [18–20], and there has been a lack of studies on flow mechanics related to constant-head pumping in unconfined aquifers. So far, existing pumping flow models in the unconfined aquifer are mainly proposed by considering (1) with and (2) without vertical flow components. With the vertical flow component, the release of gravity storage takes a long time to complete, which further leads to the formation of an unsaturated region above the hydraulic head and to the vertical replenishment of the aquifer [21]. Without the vertical flow component, the flow is horizontal and uniform everywhere in a vertical section. Gravity storage is considered to be released instantaneously. The solution considering the vertical recharge flow is more accurate than that without vertical flow. However, such solutions are extremely complex and have empirical parameters that cannot be tested, which inhibits their applicability. In a constant-head test with a small drawdown inside the pumping well or long enough pumping time, the influence of the vertical flow is limited. In this case, the use of the Dupuit assumption assuming that the gravity storage is an instantaneous release, is reasonable [22,23]. The Dupuit assumption insists that the effect of vertical flow can be ignored when the drawdown of the unconfined aquifer changes slowly and considers that all recharge flow comes from the horizontal direction. Hence, it can be used to simplify the unconfined flow problem and makes it analytically tractable [23]. Practically, the use of flow modeling by considering the Dupuit assumption is preferred to meet the engineering requirements when the drawdown is significantly smaller than the initial hydraulic head in the unconfined aquifer [24–27].

Otherwise, previous studies have generally assumed that the non-Darcian flow happens in the entire pumped aquifer [17]. Such an assumption is doubtful by field observations [28]. Theoretically speaking, at the beginning of the pumping, the specific discharge nearby the pumping well is sufficiently large, which cannot be ignored owing to an intensive decline of the hydraulic head. A sufficiently large specific discharge can make the Reynolds number greater than the critical Reynolds number, suggesting the presence of a non-Darcian flow. As the radial distance increases, the Reynolds number gradually decreased with the specific discharge. Thus, it can further result in the conversion from non-Darcian flow to Darcian one, indicating the development of a two-region flow in the pumped aquifer [28–30]. So far, the mechanics of such two-region flow by constant-head tests in an unconfined aquifer have remained unclearly.

In order to address the issues mentioned above, this paper proposes an analytical two-region, non-Darcian and Darcian, model for the flow induced by the constant-head pumping test in an unconfined aquifer when the drawdown inside the pumping well is small. Izbash's equation is used to depict the relationship between the specific discharge and hydraulic gradient for mathematical modeling purposes. The solution is derived using the Boltzmann transform, and the Dupuit assumption can make the equation more concise. The acceptability of the two-region model is verified by comparing it with the numerical solution of COMSOL Multiphysics and the measured data from a constant-head pumping in Wisconsin. Such investigation on the mechanics of the two-region flow by constant-head

tests in an unconfined aquifer has significant engineering values, which can provide a concise and reliable method for solving environmental damage in landfills.

2. Problem Statement

Figure 1 shows a schematic of the constant-head pumping test in an unconfined aquifer considering two-region, non-Darcian and Darcian, flow. Since the hydraulic gradient near the pumping well is usually large, a faster specific discharge can make the Reynolds number greater than the critical Reynolds number, which further converts this region of the Darcian pattern into a non-Darcian pattern. Such non-Darcian turbulence effect is diminished with distance from the pumping well. Therefore, the assumption of two-region flow is preferred to simulate the pumping flow under the influence of such non-Darcian turbulence. For convenience, the regions of the non-Darcian pattern and Darcian pattern are hereinafter referred to as the region N and region D, respectively. The assumptions of the mathematical model are mainly mentioned as follows: (1) the aquifer is unconfined, homogeneous, and isotropic; the initial hydraulic head is identical in the entire aquifer; (2) the pumping well fully penetrates the unconfined aquifer and the hydraulic head inside the pumping well is invariable from the start of pumping; (3) the finite non-Darcian region, such as the region N, is mainly developed around the pumping well, and the semi-infinite Darcian region, such as the region D, is sequentially located near the region N; and (4) the radius of the wellbore is the same as the effective radius with a fixed positive number [31].

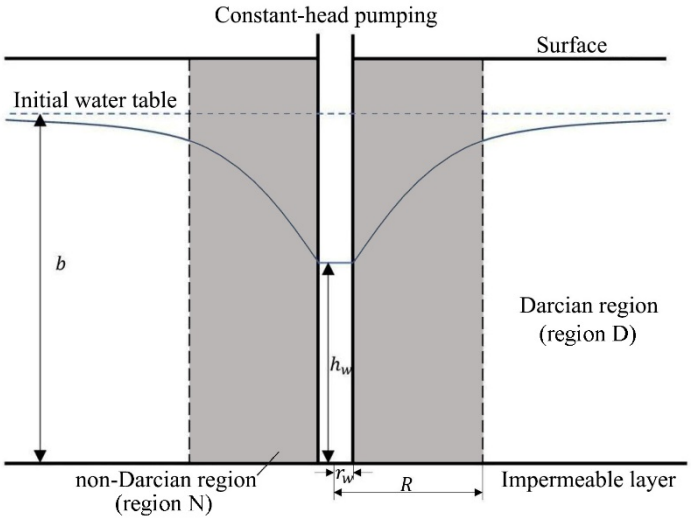

Figure 1. Schematic of the constant-head test in an unconfined aquifer considering the two-region transform.

Based on the law of mass conservation and Dupuit assumption, the Boussinesq equation is used to describe the pumping flow in the regions N and D as Equations (1a) and (1b), respectively.

$$\frac{\partial q_1}{\partial r} + \frac{q_1}{r} = \frac{S_1}{h_1}\frac{\partial h_1}{\partial t}, \tag{1a}$$

$$\frac{\partial q_2}{\partial r} + \frac{q_2}{r} = \frac{S_2}{h_2}\frac{\partial h_2}{\partial t}, \tag{1b}$$

where q_1 and q_2 are the specific discharges in the regions N and D [L/T], respectively, $h_1(r,t)$ and $h_2(r,t)$ are the hydraulic heads in the regions N and D [L], respectively, and the above parameters are functions of time t [T] and distance r [L] from the pumping well. S_1 and S_2 are the storativity in the regions N and D, respectively. Considering that the values of storativity are determined by the aquifer medium, in general, it should be considered that $S_1 = S_2$.

Assuming that the groundwater in the regions N and D are under the non-Darcian and Darcian conditions, respectively [28], the specific discharges in the regions N and D are expressed using the Izbash's and Darcian equations, respectively.

$$q_1 = \left(-K_1 \frac{\partial h_1}{\partial r}\right)^{\frac{1}{n_1}}, \tag{2a}$$

$$q_2 = -K_2 \frac{\partial h_2}{\partial r}, \tag{2b}$$

where K_1 is the quasi-hydraulic conductivity in the region N [L^{n_1}/T^{n_1}], K_2 is the hydraulic conductivity in the region D [L/T], and n_1 is the non-Darcian coefficient representing the turbulent flow in the region N. Based on Izbash's equation, the flow is non-Darcian when $1 < n_1 \leq 2$, which means that the Reynolds number of the flow is greater than the critical Reynolds number [24]. When $n_1 = 1$, Equation (2a) becomes an expression of Darcian's law, and K_1 is the hydraulic conductivity [12]. The values of K_1 and n_1 are both constant empirical parameters, which can be evaluated by approximating aquifer drawdown-time measured data [32–36]. For example, Sen [34] derived the value of the non-Darcian coefficient, n_1, by an automatic program according to Simpson's rule through a set of constant rate pumping data in a leakage aquifer located in the Kingdom of Saudi Arabia, and the quasi-hydraulic conductivity, K_1, was obtained by further substituting other parameters into the proposed analytical solution. This method has been widely used in non-Darcian studies, and its reliability can be assured [28,32–35,37].

The initial condition before pumping starts is

$$\lim_{t \to 0} h_1 = \lim_{t \to 0} h_2 = b, \tag{3}$$

where b is the initial hydraulic head [L].

In the pumping test without the wellbore storage, the boundary conditions representing the fully penetrating well are as follows:

$$\lim_{r \to r_w} h_1 = h_w, \tag{4}$$

$$\lim_{r \to r_w} 2\pi r h_w \left(K_1 \frac{\partial h_1}{\partial r}\right)^{\frac{1}{n_1}} = -Q, \tag{5}$$

where r_w is the effective radius of the pumping well [L], h_w is the constant hydraulic head inside the pumping well [L], and Q is the flow rate changing with time [L^3/T].

The far-field boundary condition is

$$\lim_{r \to \infty} h_1 = b. \tag{6}$$

The conversion interface between the regions N and D is assumed to be located in the radial distance with $r = R$, and the boundary conditions for the flow continuity are obtained as follows:

$$q_1|_{r \to R} = q_2|_{r \to R}, \tag{7}$$

$$h_1|_{r \to R} = h_2|_{r \to R}, \tag{8}$$

where R is the distance of the conversion interface between the regions N and D [L], which is a function that varies with time.

3. Solution Derivation

Substituting Equations (2a) and (2b) into Equations (1a) and (1b) yields

$$\frac{\partial^2 h_1}{\partial r^2} + \frac{n_1}{r}\frac{\partial h_1}{\partial r} = \frac{S_1}{h_1}\frac{n_1}{K_1^{\frac{1}{n_1}}}\left(-\frac{\partial h_1}{\partial r}\right)^{\frac{n_1-1}{n_1}}\frac{\partial h_1}{\partial t}, \tag{9a}$$

$$\frac{\partial^2 h_2}{\partial r^2} + \frac{1}{r}\frac{\partial h_2}{\partial r} = \frac{S_2}{h_2 K_2}\frac{\partial h_2}{\partial t}. \tag{9b}$$

The flow rate in region N is assumed to be equal to the specific discharge multiplied by the discharge section area as described in the following equation.

$$Q \approx -Aq_1 = 2\pi r h_1\left(-K_1\frac{\partial h_1}{\partial r}\right)^{\frac{1}{n_1}}, \tag{9c}$$

where $q_1 = \left(K_1\frac{\partial h_1}{\partial r}\right)^{\frac{1}{n_1}}$ is the specific discharge [L/T], and $A = 2\pi r h_1$ is the discharge section area [L^2]. To simplify the derivation of the solution, the items of $\frac{S_1}{h_1}\frac{n_1}{K_1^{\frac{1}{n_1}}} \approx \frac{S_1}{b}\frac{n_1}{K_1^{\frac{1}{n_1}}}$, $\frac{S_2}{h_2 K_2} \approx \frac{S_2}{bK_2}$ and $2\pi r h_1 \approx 2\pi r b$ are introduced to Equations (9a), (9b), and (9c), respectively, which can be used to linearize the Dupuit equation. The errors caused by such approximations have been found to be relatively small. Hence, they can be neglected for modeling purposes [36]. Thus, Equations (9a), (9b), and (9c) can be approximately written as

$$\frac{\partial^2 h_1}{\partial r^2} + \frac{n_1}{r}\frac{\partial h_1}{\partial r} = \frac{S_1}{b}\frac{n_1}{K_1^{\frac{1}{n_1}}}\left(-\frac{\partial h_1}{\partial r}\right)^{\frac{n_1-1}{n_1}}\frac{\partial h_1}{\partial t}, \tag{10a}$$

$$\frac{\partial^2 h_2}{\partial r^2} + \frac{1}{r}\frac{\partial h_2}{\partial r} = \frac{S_2}{bK_2}\frac{\partial h_2}{\partial t}, \tag{10b}$$

$$\frac{\partial h_1}{\partial r} = -\frac{\left(\frac{Q}{2\pi r b}\right)^{n_1}}{K_1}. \tag{10c}$$

Combining Equations (10a) with (10c), the governing equations in the regions N and D are expressed as Equations (11a) and (11b), respectively.

$$\frac{\partial^2 h_1}{\partial r^2} + \frac{n_1}{r}\frac{\partial h_1}{\partial r} = \varepsilon_1 r^{1-n_1} Q^{n_1-1}\frac{\partial h_1}{\partial t}, \tag{11a}$$

$$\frac{\partial^2 h_2}{\partial r^2} + \frac{1}{r}\frac{\partial h_2}{\partial r} = \varepsilon_2\frac{\partial h_2}{\partial t}, \tag{11b}$$

where $\varepsilon_1 = \frac{S_1}{b}\frac{n_1}{K_1}\left(\frac{1}{2\pi b}\right)^{n_1-1}$ and $\varepsilon_2 = \frac{S_2}{bK_2}$.

The analytical solution of the mathematical model with Equations (3), (7), and (11a) for the region N and with Equations (5), (6), (8), and (11b) for the region D are derived using the Boltzmann transformation method. The detailed derivation is provided in Appendix A, by which the expressions of the hydraulic head in regions N and D can be obtained as Equations (12a) and (12b), respectively.

$$h_1 = b - F_1\int_{0.1}^{\eta} m^{-1}\exp\left(-\frac{\varepsilon_1 r^{1-n_1}}{4}m^2\right)\mathrm{d}m + F_2 W(v_R) + F_1\int_{0.1}^{\eta_R} m^{-1}\exp\left(-\frac{\varepsilon_1 R^{1-n_1}}{4}m^2\right)\mathrm{d}m, \tag{12a}$$

$$h_2 = b - F_2 W(v), \tag{12b}$$

where

$$F_1 = \frac{Q^{n_1} \exp\left(\frac{\varepsilon_1 {r_w}^{1-n_1}}{4} {\eta_w}^2\right) r^{1-n_1}}{(2\pi)^{n_1} {h_w}^{n_1-1} b K_1}, \tag{13a}$$

$$F_2 = \frac{Q \exp\left(\frac{\varepsilon_1 {r_w}^{1-n_1}}{4n_1} {\eta_w}^2\right)}{4\pi {h_w}^{\frac{n_1-1}{n_1}} b^{\frac{1}{n_1}} K_2 \exp\left(-\frac{\varepsilon_2}{4}\eta_R{}^2\right)} \exp\left(-\frac{\varepsilon_1 R^{1-n_1}}{4n_1} {\eta_R}^2\right), \tag{13b}$$

$$v = \frac{\varepsilon_2}{4}\eta^2, \tag{13c}$$

$$v_R = \frac{\varepsilon_2}{4}{\eta_R}^2, \tag{13d}$$

$$\eta = r t^{-\frac{1}{2}}, \tag{13e}$$

$$\eta_R = R t^{-\frac{1}{2}}, \tag{13f}$$

$$\eta_w = r_w t^{-\frac{1}{2}}, \tag{13g}$$

$$W(x) = \int_x^\infty \frac{e^{-y}}{y} dy. \tag{13h}$$

The constant-head pumping test can make the hydraulic head near the pumping well declines rapidly at the early pumping time and approaches to h_w in a short time. After that, the magnitude of the hydraulic head change can slow down considerably. Therefore, the proposed analytical solution based on the Dupuit assumption is acceptable except for a short period of time when the pumping starts.

In a constant-head test, since the turbulence of the flow can be weakened with increasing radial distance from the pumping well, the region N can be defined as the area with Reynolds number, Re, greater than the critical Reynolds number, Re_c, and the R value can be determined by investigating the position of $Re = Re_c|_{r \to R}$ at any interesting time. In addition, it should be noted that the proposed solution can also be used to assess the drawdown behavior of pure Darcian flow with $R = r_w$ and pure non-Darcian flow with $R = \infty$. The equation for calculating the Reynolds number is as follows [28]:

$$Re = \frac{qd}{v}, \tag{14a}$$

where Re is the Reynolds number, q is the specific discharge [L/T], and d is the characteristic diameter of the medium [L]. v is the kinematic viscosity of water [L^2/T], the value of which is generally 1×10^6 m^2/s. Substituting Equation (12b) into Equation (14a), the critical Reynolds number at the conversion interface of Darcian and non-Darcian regions can be obtained as

$$Re_c = \frac{d}{v}[b - F_2 W(v)]|_{r \to R}, \tag{14b}$$

where Re_c is the critical Reynolds number, which is generally considered that $Re_c = 10$. Therefore, in order to determine the value of R, Equation (14b) can be rewritten as follows:

$$\frac{QW\left(\frac{\varepsilon_2 R^2}{4t}\right)}{\exp\left(-\frac{\varepsilon_2 R^2}{4t}\right)} \exp\left(-\frac{\varepsilon_1 R^{3-n_1}}{4n_1 t}\right) = \frac{4\pi {h_w}^{\frac{n_1-1}{n_1}} b^{\frac{1}{n_1}} K_2 \left(b - \frac{v}{d} Re_c\right)}{\exp\left(\frac{\varepsilon_1 {r_w}^{1-n_1}}{4n_1} {\eta_w}^2\right)}. \tag{15a}$$

Equation (15a) is an implicit function of R and Q at the time t constant. Based on Equations (4) and (12a), another implicit expression for the interface distance R and discharge rate Q can be obtained as

$$\left[b - h_w + F_1 \int_{0.1}^{\eta_w} m^{-1} \exp\left(-\frac{\varepsilon_1 {r_w}^{1-n_1}}{4} m^2\right) \mathrm{d}m - F_2 W(v_R) - F_1 \int_{0.1}^{\eta_R} m^{-1} \exp\left(-\frac{\varepsilon_1 R^{1-n_1}}{4} m^2\right) \mathrm{d}m\right]|_{r \to r_w} = 0. \tag{15b}$$

Then, the interface distance R and pumping rate Q at each given time point t is assumed to be the root of Equations (15a) and (15b), which can be solved using the built-in module called Equations and System Solver in MATLAB.

Constant-head tests are often used to investigate the characteristics of hydraulic parameters in confined and unconfined aquifers. In the section, a model for the constant-head pumping flow in the confined aquifer can be degenerated based on the proposed solution by Equations (12a,b) and (15a,b). With the Dupuit assumption, the main difference between the models in the unconfined and the confined aquifers is depicted in the boundary condition at the pumping wellbore, which is formulated in the confined aquifer as

$$\lim_{r \to r_w} 2\pi r B \left(K_1 \frac{\partial h_1}{\partial r} \right)^{\frac{1}{n_1}} = -Q, \tag{16}$$

where B is the thickness of the confined aquifer [L].

Replacing Equation (5) with Equation (16), the solutions of the hydraulic head in regions N and D at the confined aquifer can be given as Equation (17a,b) by the same derivation method of Equation (12a,b), respectively.

$$h_1 = h_0 - F_3 \int_{0.1}^{\eta} m^{-1} \exp\left(-\frac{\varepsilon_1 r^{1-n_1}}{4} m^2 \right) \mathrm{d}m + F_4 W(v_R) + F_3 \int_{0.1}^{\eta_R} m^{-1} \exp\left(-\frac{\varepsilon_1 R^{1-n_1}}{4} m^2 \right) \mathrm{d}m, \tag{17a}$$

$$h_2 = h_0 - F_4 W(v), \tag{17b}$$

and

$$F_3 = \frac{Q^{n_1} \exp\left(\frac{\varepsilon_1 {r_w}^{1-n_1}}{4} {\eta_w}^2 \right) r^{1-n_1}}{(2\pi)^{n_1} B^{n_1} K_1}, \tag{18a}$$

$$F_4 = \frac{Q \exp\left(\frac{\varepsilon_1 {r_w}^{1-n_1}}{4n_1} {\eta_w}^2 \right)}{4\pi B K_2 \exp\left(-\frac{\varepsilon_2}{4} {\eta_R}^2 \right)} \exp\left(-\frac{\varepsilon_1 R^{1-n_1}}{4n_1} {\eta_R}^2 \right), \tag{18b}$$

where h_0 is the initial hydraulic head in the confined aquifer [L].

Similarly, substituting Equation (17a,b) into Equations (4) and (14a,b) can obtain two implicit functions as

$$\frac{QW\left(\frac{\varepsilon_2 R^2}{4t} \right)}{\exp\left(-\frac{\varepsilon_2 R^2}{4t} \right)} \exp\left(-\frac{\varepsilon_1 R^{3-n_1}}{4n_1 t} \right) = \frac{4\pi B^{\frac{n_1-1}{n_1}} {h_0}^{\frac{1}{n_1}} K_2 \left(h_0 - \frac{v}{d} Re_c \right)}{\exp\left(\frac{\varepsilon_1 {r_w}^{1-n_1}}{4n_1} {\eta_w}^2 \right)}. \tag{19a}$$

$$\left[h_0 - B + F_3 \int_{0.1}^{\eta_w} m^{-1} \exp\left(-\frac{\varepsilon_1 {r_w}^{1-n_1}}{4} m^2 \right) \mathrm{d}m - F_4 W(v_R) - F_3 \int_{0.1}^{\eta_R} m^{-1} \exp\left(-\frac{\varepsilon_1 R^{1-n_1}}{4} m^2 \right) \mathrm{d}m \right] \Bigg|_{r \to r_w} = 0. \tag{19b}$$

Equations (19a) and (19b) can be solved by MATLAB software to obtain the flow rate Q and the distance of interface R at each given time point.

4. Verification

In order to investigate the acceptability of the proposed analytical solution, Case A in Table 1 is conducted to compare the simulation results of the hydraulic head and development of region N by the analytical solution with that of the numerical solution. In addition, a series of drawdown data from the constant-head pumping test in Wisconsin, USA, has been presented to demonstrate the reliability of the proposed solution in practice.

Table 1. Parameter values for hypothetical cases.

Parameters	Case A	Case B	Case C
h_w (m)	9	7, 8, 9	9
K_1 $\left[(\mathrm{m/day})^{n_1}\right]$	1.1	1.1	1.1
K_2 (m/day)	1.1	1.1	1.1
n_1	1.1	1.2	1, 1.2, 1.4
S_1	0.01	0.01	0.01
S_2	0.01	0.01	0.01
b (m)	12	10	12
r_w (m)	0.2	0.2	0.2
r (m)	3	5	2
d (mm)	0.3	0.3	0.3

The numerical solution is performed by using the finite element method via COMSOL Multiphysics, which has proven to be one of the most useful software for multiphysics simulations [38]. The finite element solution is derived based on Equations (3), (4), and (9a) for the region N and Equations (3), (6), and (9b) for the region D. It should be noted that the distance of infinity boundary in Equation (6) is depicted by $r = 2000$ m in the COMSOL solution. A MATLAB program is developed to automatically solve the proposed analytical solutions of Equations (12a,b) and (15a,b). A hypothetical unconfined aquifer is assumed to be a sandy medium. Generally, the range of storativity in an unconfined aquifer is 0.01–0.3, and the hydraulic conductivity of fine sand unconfined aquifer ranges from 1 to 5 $\mathrm{m}^3/\mathrm{day}$ [23]. Hence, a set of parameters is reasonably selected for Case A, as listed in Table 1. Considering the requirement of the Dupuit assumption, the drawdown inside the pumping well needs to take a relatively smaller value so that the parameters of $b = 12$ m and $h_w = 9$ m are chosen.

The comparison of the hydraulic head−time curves of the two-region flow (R is a variable), pure Darcian flow ($R = 0.2$ m), and pure non-Darcian flow ($R = \infty$) are demonstrated in Figure 2. The pure non-Darcian COMSOL solution is approximated by $R = 2000$ m. It is noticed that K_1 and S_1 are meaningless for the simulation of pure Darcian flow, when K_2 and S_2 are meaningless for the simulation of pure non-Darcian flow. Such comparison clearly indicates that the deviations between the simulation results by both proposed and finite element solutions are small under all three flow conditions. Certain deviations in the first hour after pumping starts are assumed to be induced by the neglect of the vertical flow of the proposed analytical solution, which can gradually disappeared with time. Such errors should be acceptable in case the drawdown inside the pumping well is relatively small. It verifies the validity of the use of the proposed analytical solution for the simulation of the hydraulic head for the two-region flow.

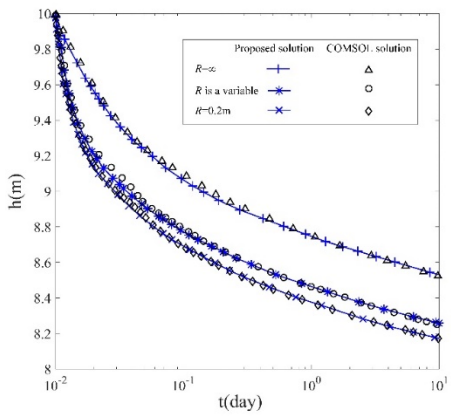

Figure 2. Comparison of the hydraulic head−time curves of analytical and numerical solutions.

Moreover, the hydraulic head of the two-region flow is found to be substantially greater than that of pure Darcian one and to be smaller than that of pure non-Darcian one (Figure 2), suggesting a negative non-Darcian effect on the decline of the hydraulic head. It is because the greater n_1 and R values lead to a greater turbulence degree in the pumped unconfined aquifer. A greater degree of turbulence means a relatively larger specific discharge so that the recharge from the far-away region can be enhanced and the release of gravity storage can be improved [15].

In order to verify the reliability of Equation (15a,b), the R–t curves based on the parameters in Case A by both analytical and numerical solutions are simulated, as shown in Figure 3. The results suggest that the fitting degree by different solutions is relatively high. Hence, the R value calculated by two implicit functions of Equation (15a,b) should be considered to be accurate. Otherwise, R value is found to be decreased with time, indicating that the influence of non-Darcian in the two-region flow is weakened as pumping continues. It is explained that after the pumping starts, the hydraulic head of the aquifer gradually declined and is approached to be h_w. Its further results in a reduction in hydraulic gradient and specific discharge. The smaller specific discharge results in a slower flow rate and smaller Reynolds number, which ultimately leads to the degeneration of region N [28]. When the pumping time is long enough, region N can disappear completely, and the two-region flow can be transformed into pure Darcian flow.

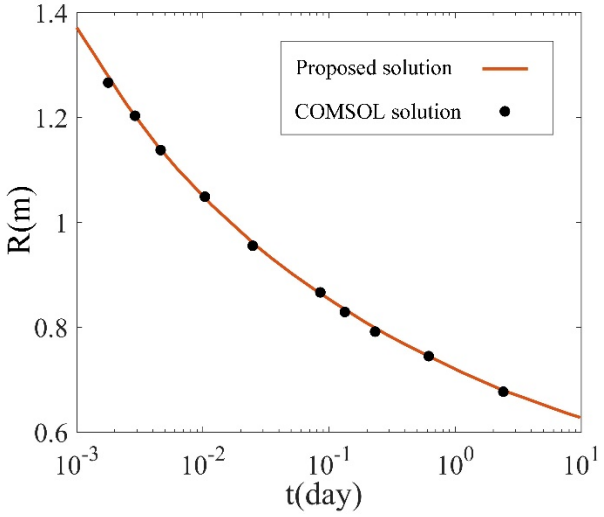

Figure 3. Comparison of the interface distance−time curve of analytical and numerical solutions.

Afterward, the constant-head pumping test in Wisconsin, USA, reported by Jones et al. [39], is used to demonstrate the engineering application of the proposed solution. The unconfined aquifer with a thickness of 2.5 m is composited of shallow weathered glacial till of low clay content and high sand content [39]. The pumping well with an effective radius of 0.051 m is fully penetrating the unconfined aquifer, of which the bottom is filled by pea gravel. During the 24-h pumping period, the hydraulic head inside the constant-head well is 1.5 m [34]. The two drawdown data series have been collected in observation wells with a radial distance of 0.87 m and 3.62 m, respectively. Based on the work from Chen and Chang [3], the ranges of gravity storage and hydraulic conductivity in the horizontal direction can be considered as 0.014–0.042 and 0.241–0.362 m/day, respectively. Therefore, after careful investigation, the best-fitting results based on Equation (12a,b) can be obtained when $S_1 = S_2 = 0.031$, $K_1 = 0.285$ m/day, $K_2 = 0.32$ m/day and $n_1 = 1.3$. The comparison curves shown in Figure 4 matched well with each other, suggesting the acceptability of the use of the proposed solution in practice. However, similar to the results in Figure 2, the simulation curves by the analytical solution rarely deviate from the measured data at the beginning of pumping, and such deviation is gradually disappeared with time. It

further verifies that the proposed solution is applicable even at a 40% relative drawdown ($\frac{b-h_w}{b} = 40\%$) inside the pumping well in the aquifer investigated.

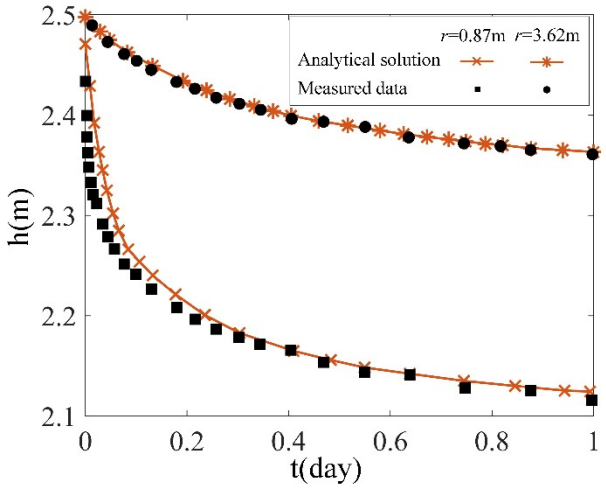

Figure 4. Comparison of the hydraulic head−time curves of the analytical solution and measured data.

5. Discussion

Accurate evaluation of the dynamic development of the pumping rate Q is vital for designing a practical constant-head test. In this section, the effect of the hydraulic head inside the pumping well, h_w, and the degree of turbulence in the non-Darcian flow, represented by n_1, on the dynamic development of the pumping rate is investigated using hypothetical case studies: Case B and Case C. The parameters for the two case studies are listed in Table 1.

Figure 5 shows the simulation results for Q–t curves ith different h_w. The results indicate that the development of Q is negatively correlated with the h_w value and it confirms the fact that a small decrease in h_w value can greatly increase the flow rate. It is due to that the flow rate is essentially caused by the hydraulic gradient resulting from the hydraulic head decline inside the pumping well. Therefore, a greater h_w means a slower specific discharge, which can lead to a lower flow rate.

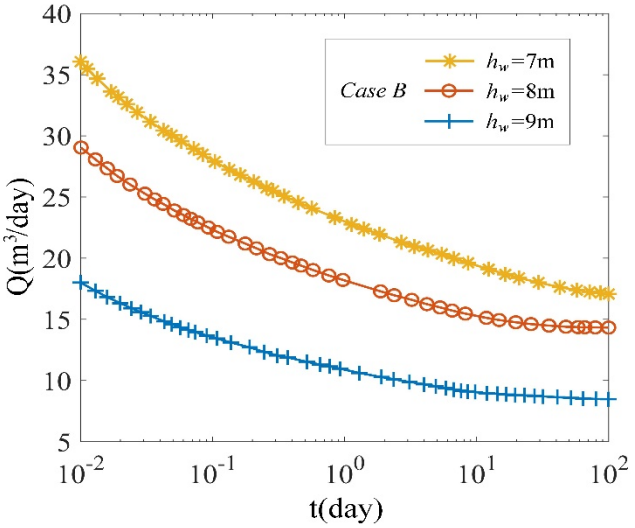

Figure 5. Dynamic development of the flow rates with different hydraulic heads inside the pumping well.

Figure 6 represents the effect of non-Darcian turbulence on the pumping flow according to Case C. The Q–t curves at a fixed radial distance $r = 2$ m are shown in Figure 6a), which indicates that the flow rate at a given time point is found to be increased by n_1 at the early pumping time. As the pumping continues, the deviations of the flow rates with different n_1 values can be decreased. Theoretically, it is understandable. The flow rate is dominated by the recharge from gravity storage, which is assumed to be equal to the specific discharge multiplied by the discharge section area as described in Equation (9c). The higher the specific discharge is, the higher the pumping rate is. Thus, at the early pumping time, the release of gravity storage of the aquifer gradually replenishes the water level nearby the pumping well, causing a greater turbulence flow with a greater n_1 value can result in a faster specific discharge and a larger flow rate in the unconfined aquifer. As the pumping continues, the range of the region N is degenerated, which further reduces the influence of n_1 and the gradual agreement of the Q–t curves.

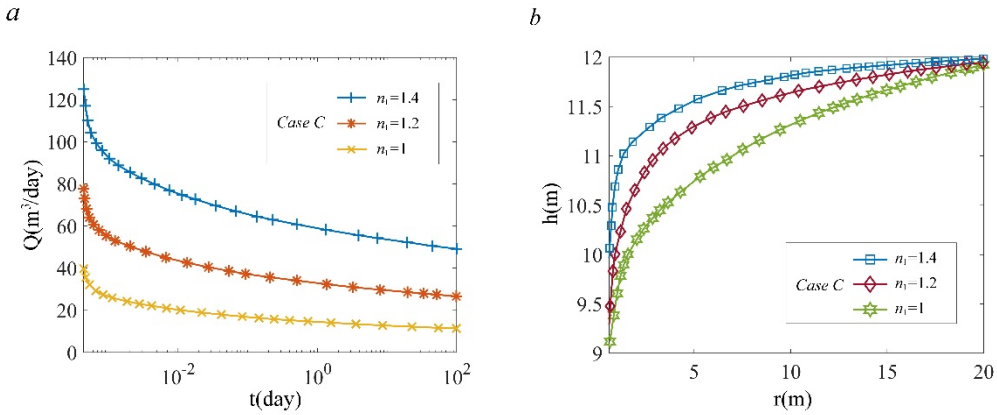

Figure 6. Dynamic development of (**a**) Q–t curves in a constant radial distance and (**b**) h–r curves at a fixed time moment with different non-Darcian coefficients.

Figure 6b presents the h–r curves at the same pumping time $t = 1$ day to investigate the development characteristics of non-Darcian turbulence with radial distance. It shows that there is a positive correlation between the non-Darcian coefficient and the hydraulic head, of which effect is suppressed at a larger radial distance. The larger n_1 value means the larger the hydraulic gradient, leading to a larger flow rate. Nearby the pumping well, the hydraulic head fluctuated greatly, but there is no unreasonable mutation, which can prove the continuity of the proposed solution.

Subsequently, a comparison of the proposed model with Li et al.'s [17] solution has been demonstrated in Figure 7. It shows the results for the proposed models in an unconfined aquifer based on Equation (12a,b), labeled as the Proposed solution in U, and in a confined aquifer based on Equation (17a,b), entitled as the Proposed solution in C. By Li et al.'s [17] hypothetical case, a set of parameters is given as $h_w = 40$ m, $r = 0.2$ m, $b = B = 20$ m and $S_1 = S_2 = 0.004$. Li et al. [17] propose a semi-analytical model for a constant-head pumping test in the confined aquifer by considering the hydraulic conductivity as a variable related exponentially with time and assuming that the pumping flow is obeyed by non-Darcian law. Therefore, to allow the proposed solution in the confined aquifer to be fully consistent with the actual situation of Li et al.'s [17] research, it can be assumed that $R = \infty$ and $K_1 = 0.006 + 0.054\mathrm{e}^{-0.05t}$ m/hr. Otherwise, in the case of $K_1 = 0.06$ m/hr and $K_2 = 0.006$ m/hr, the hydraulic head increment−time curve for the two-region flow is also simulated based on the proposed solution of Equations (12a,b) and (15a,b), which can be used to demonstrate the difference between the proposed model and Li et al.'s [17] work.

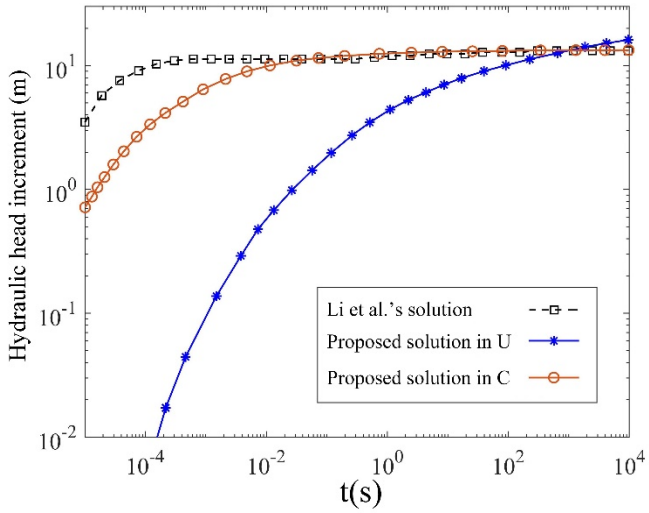

Figure 7. Comparison of the hydraulic head increment−time curves of proposed and Li et al.'s [17] solutions.

In Figure 7, the hydraulic head increment−time curves for the three models show a significant deviation, and the use of the proposed solution in the unconfined aquifer can yield a higher hydraulic head when the pumping time is long enough. It is because the wetted cross-section for pumping flow at the constant-head test in an unconfined aquifer is larger than in a confined aquifer ($h \geq b$). It means that the hydraulic head can increase more rapidly. The result of the proposed solution in the confined aquifer is fitted with that of Li et al. [17] after 0.1 s, which indicates that the analytical solution obtained by Equation (17a,b) is applicable in the confined aquifer. Otherwise, it is noted that the pumping rate is set to be constant for simplified calculations by Li et al. [17], which is assumed to introduce errors for hydraulic head assessment at the early pumping time. It further results in the difference between the two curves before 0.1 s after the pumping starts. The comparison demonstrates that the analytical models can be used to characterize the constant-head test in both confined and unconfined aquifers.

6. Conclusions

This paper proposes an analytical solution for two-region flow induced by constant-head pumping tests. Based on the Dupuit assumption, the proposed model is available for an unconfined aquifer when the constant drawdown inside the pumping well is small. The nonlinear relationship between the specific discharge and hydraulic gradient in the non-Darcian region is expressed using Izbash's equation, and the analytical solution is derived using the Boltzmann transform. The reliability of the analytical solution is verified through a numerical model via COMSOL Multiphysics and a set of hydraulic head−time data in a pumping test in Wisconsin. The non-Darcian effect on both the hydraulic head decline and dynamic development of the pumping rate is investigated during constant-head tests. The main conclusions are as follows:

(1) The proposed analytical solution can be used for drawdown simulations in the cases of two-region, pure Darican, and pure non-Darcian flows induced by constant-head pumping tests. In the case of the two-regions flow, the proposed solution can also be used for the assessment of the dynamic development of the pumping flow rate and non-Darcian region.

(2) The neglect of the finite expansion of the non-Darcian region may introduce errors to the hydraulic head simulation of a two-region flow. The turbulence flow in the finite non-Darcian region can lead to positive and negative deviations of the hydraulic head−time curves from pure non-Darcian and pure Darcian flows, respectively. The range of non-Darcian regions can decrease with time.

(3) Using Izbash's equation, the transient pumping rate−time behavior can be significantly controlled by the hydraulic head inside the pumping well h_w and non-Darcian coefficient n_1. The decrease in h_w value or increase of n_1 value can improve the pumping rate at a given time point. Such effect is gradually weakened and be disappeared towards the end of pumping time.

Consequently, the proposed model provides a concise method for quantitatively investigating the good hydraulics around the pumping well under the combined effect of both non-Darcian and Darcian flows and offers a theoretical basis for designing the pumping rate during the constant-head test.

Author Contributions: Conceptualization, Y.Z. and L.X.; methodology, L.X.; software, Y.Z.; validation, Y.Z.; investigation, L.X.; resources, L.X.; writing—original draft preparation, Y.Z.; funding acquisition, L.X.; writing—review and editing, L.X. and Y.Z.; supervision, L.X. and Y.Z. All authors have read and agreed to the published version of the manuscript.

Funding: This research was funded by [National Natural Science Foundation of China] grant number [2017YFC0405900], [Natural Science Foundation of Guangxi] grant number [2018GXNSFAA138042] and [Hebei High-level Talent Funding Project] grant number [B2018003016].

Institutional Review Board Statement: Not applicable.

Informed Consent Statement: Not applicable.

Data Availability Statement: The data that support the findings of this study are available from the corresponding author upon reasonable request.

Conflicts of Interest: The authors declare no conflict of interest.

Appendix A

The initial-value problems of the mathematical model of Equations (3), (7), and (11a) for the region N and of Equations (5), (6), (8), and (11b) for the region D are solved by Boltzmann transform as following. To convert Equation (11a,b) from partial differential equations to ordinary differential equations, a similar item is introduced as

$$\eta = rt^{-\frac{1}{2}}, \tag{A1}$$

where η is a similar item of radius r and time t. Using Equation (A1), Equations (A2), (A3) and (A4) can be obtained in terms of η.

$$\frac{\partial h_n}{\partial r} = t^{-\frac{1}{2}} \frac{dh_n}{d\eta}, \tag{A2}$$

$$\frac{\partial^2 h_n}{\partial r^2} = t^{-1} \frac{d^2 h_n}{d\eta^2}, \tag{A3}$$

$$\frac{\partial h_n}{\partial t} = -\frac{1}{2} r t^{-\frac{3}{2}} \frac{dh_n}{d\eta}, \tag{A4}$$

where h_n represents the similarity items of h_1 or h_2.

Thus, Equations (11a) and (11b) can be rewritten as

$$\frac{d^2 h_1}{d\eta^2} + \left(\frac{n_1}{\eta} + \frac{\varepsilon_1 Q^{n_1 - 1} r^{1 - n_1}}{2} \eta \right) \frac{dh_1}{d\eta} = 0, \tag{A5}$$

$$\frac{d^2 h_2}{d\eta^2} + \left(\frac{1}{\eta} + \frac{\varepsilon_2}{2} \eta \right) \frac{dh_2}{d\eta} = 0. \tag{A6}$$

After variable separations and integration of Equations (A5) and (A6), the item of $\frac{dh_1}{d\eta}$ and $\frac{\mathrm{d}h_2}{\mathrm{d}\eta}$ can be expressed as Equations (A7) and (A8), respectively.

$$\frac{dh_1}{d\eta} = D_1\eta^{-n_1}\exp\left(-\frac{\varepsilon_1 Q^{n_1-1}r^{1-n_1}}{4}\eta^2\right), \tag{A7}$$

$$\frac{\mathrm{d}h_2}{\mathrm{d}\eta} = D_2\eta^{-1}\exp\left(-\frac{\varepsilon_2}{4}\eta^2\right), \tag{A8}$$

where D_1 and D_2 are integration constants. Similarly, substituting Equations (A2), (A3), and (A4) into Equations (3), (5), (6), (7), and (9), the initial and boundary conditions can be established in term of η as

$$h_2(\eta \to \infty) = b, \tag{A9}$$

$$\lim_{\eta\to\eta_w} 2\pi bK_1\left(\frac{Q}{2\pi r_w h_w}\right)^{1-n_1}\eta\frac{dh_1}{d\eta} = -Q, \tag{A10}$$

$$\frac{\mathrm{d}h_1}{\mathrm{d}\eta}\Big|_{r\to R} = \frac{{K_2}^{n_1}}{K_1}t^{-\frac{1}{2}(n_1-1)}\left(\frac{\mathrm{d}h_2}{\mathrm{d}\eta}\right)^{n_1}\Big|_{r\to R}, \tag{A11}$$

$$h_1|_{r\to R} = h_2|_{r\to R}. \tag{A12}$$

Combining Equation (A10) with Equation (A7), the item of D_1 can be determined and Equation (A7) can be given as

$$\frac{dh_1}{d\eta} = -\frac{Q^{n_1}t^{\frac{1-n_1}{2}}\exp\left(\frac{\varepsilon_1 Q^{n_1-1}{r_w}^{1-n_1}}{4}{\eta_w}^2\right)}{(2\pi)^{n_1}{h_w}^{n_1-1}bK_1}\eta^{-n_1}\exp\left(-\frac{\varepsilon_1 Q^{n_1-1}r^{1-n_1}}{4}\eta^2\right). \tag{A13}$$

Applying Equations (A13) and (A11) to Equation (A8), the item of D_2 can be assessed and Equation (A8) can be obtained as

$$\frac{dh_2}{d\eta} = \frac{Q\exp\left(\frac{\varepsilon_1 Q^{n_1-1}{r_w}^{1-n_1}}{4n_1}{\eta_w}^2\right)}{2\pi{h_w}^{\frac{n_1-1}{n_1}}b^{\frac{1}{n_1}}K_2\exp\left(-\frac{\varepsilon_2}{4}{\eta_R}^2\right)}\exp\left(-\frac{\varepsilon_1 Q^{n_1-1}R^{1-n_1}}{4n_1}{\eta_R}^2\right)\eta^{-1}\exp\left(-\frac{\varepsilon_2}{4}\eta^2\right). \tag{A14}$$

After variable separations and integration of Equation (A13), the equation of hydraulic head in the region N is derived as

$$h_1 = \frac{Q^{n_1}\exp\left(\frac{\varepsilon_1 Q^{n_1-1}{r_w}^{1-n_1}}{4}{\eta_w}^2\right)r^{1-\mathrm{n}_1}}{(2\pi)^{n_1}{h_w}^{n_1-1}bK_1}\int_{0.1}^{\eta} m^{-1}\exp\left(-\frac{\varepsilon_1 Q^{n_1-1}r^{1-n_1}}{4}m^2\right)\mathrm{d}m + B_1. \tag{A15}$$

Similarly, after separation and integration of Equation (A14), the governing equation with an arbitrary constant in the region D is

$$h_2 = \frac{Q\exp\left(\frac{\varepsilon_1 Q^{n_1-1}{r_w}^{1-n_1}}{4n_1}{\eta_w}^2\right)}{2\pi{h_w}^{\frac{n_1-1}{n_1}}b^{\frac{1}{n_1}}K_2\exp\left(-\frac{\varepsilon_2}{4}{\eta_R}^2\right)}\exp\left(-\frac{\varepsilon_1 Q^{n_1-1}R^{1-n_1}}{4n_1}{\eta_R}^2\right)\int_{0.1}^{\eta} m^{-1}\exp\left(-\frac{\varepsilon_2}{4}m^2\right)\mathrm{d}m + B_2, \tag{A16}$$

where η_R is defined as $Rt^{-\frac{1}{2}}$, η_w is depicted as $r_w t^{-\frac{1}{2}}$, B_1 and B_2 are integration constants.

Substituting Equation (A9) into Equation (A16), the arbitrary constant of B_2 can be expressed as

$$B_2 = b - \frac{Q\exp\left(\frac{\varepsilon_1 Q^{n_1-1}{r_w}^{1-n_1}}{4n_1}{\eta_w}^2\right)}{2\pi{h_w}^{\frac{n_1-1}{n_1}}b^{\frac{1}{n_1}}K_2\exp\left(-\frac{\varepsilon_2}{4}{\eta_R}^2\right)}\exp\left(-\frac{\varepsilon_1 Q^{n_1-1}R^{1-n_1}}{4n_1}{\eta_R}^2\right)\int_{0.1}^{\infty} m^{-1}\exp\left(-\frac{\varepsilon_2}{4}m^2\right)\mathrm{d}m. \tag{A17}$$

Hence, Equation (A16) can be obtained as

$$h_2 = b - \frac{Q\exp\left(\frac{\varepsilon_1 Q^{n_1-1} {r_w}^{1-n_1}}{4n_1}{\eta_w}^2\right)}{2\pi {h_w}^{\frac{n_1-1}{n_1}} b^{\frac{1}{n_1}} K_2 \exp\left(-\frac{\varepsilon_2}{4}{\eta_R}^2\right)} \exp\left(-\frac{\varepsilon_1 Q^{n_1-1} R^{1-n_1}}{4n_1}{\eta_R}^2\right) \int_{\eta}^{\infty} m^{-1}\exp\left(-\frac{\varepsilon_2}{4}m^2\right) \mathrm{d}m. \tag{A18}$$

Substituting Equations (A15) and (A18) into Equation (A12), the item of B_1 can be evaluated as

$$B_1 = b - \frac{Q\exp\left(\frac{\varepsilon_1 Q^{n_1-1} {r_w}^{1-n_1}}{4n_1}{\eta_w}^2\right)}{2\pi {h_w}^{\frac{n_1-1}{n_1}} b^{\frac{1}{n_1}} K_2 \exp\left(-\frac{\varepsilon_2}{4}{\eta_R}^2\right)} \exp\left(-\frac{\varepsilon_1 Q^{n_1-1} R^{1-n_1}}{4n_1}{\eta_R}^2\right) \int_{\eta_R}^{\infty} m^{-1}\exp\left(-\frac{\varepsilon_2}{4}m^2\right) \mathrm{d}m -$$

$$\frac{Q^{n_1}\exp\left(\frac{\varepsilon_1 Q^{n_1-1} {r_w}^{1-n_1}}{4}{\eta_w}^2\right) r^{1-\mathrm{n}_1}}{(2\pi)^{n_1} {h_w}^{n_1-1} b K_1} \int_{0.1}^{\eta_R} m^{-1}\exp\left(-\frac{\varepsilon_1 Q^{n_1-1} r^{1-n_1}}{4}m^2\right) \mathrm{d}m. \tag{A19}$$

Combining Equation (A19) with Equation (A15) leads to

$$h_1 = \frac{Q^{n_1}\exp\left(\frac{\varepsilon_1 Q^{n_1-1} {r_w}^{1-n_1}}{4}{\eta_w}^2\right) r^{1-\mathrm{n}_1}}{(2\pi)^{n_1} {h_w}^{n_1-1} b K_1} \int_{0.1}^{\eta} m^{-1}\exp\left(-\frac{\varepsilon_1 Q^{n_1-1} r^{1-n_1}}{4}m^2\right) \mathrm{d}m + [b - \frac{Q\exp\left(\frac{\varepsilon_1 Q^{n_1-1} {r_w}^{1-n_1}}{4n_1}{\eta_w}^2\right)}{2\pi {h_w}^{\frac{n_1-1}{n_1}} b^{\frac{1}{n_1}} K_2 \exp\left(-\frac{\varepsilon_2}{4}{\eta_R}^2\right)}$$

$$\exp\left(-\frac{\varepsilon_1 Q^{n_1-1} R^{1-n_1}}{4n_1}{\eta_R}^2\right) \int_{\eta_R}^{\infty} m^{-1}\exp\left(-\frac{\varepsilon_2}{4}m^2\right) \mathrm{d}m - \frac{Q^{n_1} t^{\frac{1-n_1}{2}}\exp\left(\frac{\varepsilon_1 Q^{n_1-1} {r_w}^{1-n_1}}{4}{\eta_w}^2\right)\left(rt^{-\frac{1}{2}}\right)^{1-\mathrm{n}_1}}{(2\pi)^{n_1} {h_w}^{n_1-1} b K_1}$$

$$\int_{0.1}^{\eta_R} m^{-1}\exp\left(-\frac{\varepsilon_1 Q^{n_1-1} R^{1-n_1}}{4}m^2\right) \mathrm{d}m]. \tag{A20}$$

For simplification, Equations (A20) and (A18) can be rewritten Equations (A21) and (A22), respectively, by introduction of a series of expressions of Equations (A23)–(A27).

$$h_1 = b + F_1 \int_{0.1}^{\eta} m^{-1}\exp\left(-\frac{\varepsilon_1 r^{1-n_1}}{4}m^2\right)\mathrm{d}m - F_2 W(v_R) - F_1 \int_{0.1}^{\eta_R} m^{-1}\exp\left(-\frac{\varepsilon_1 R^{1-n_1}}{4}m^2\right)\mathrm{d}m, \tag{A21}$$

$$h_2 = b - F_2 W(v), \tag{A22}$$

and

$$F_1 = \frac{Q^{n_1}\exp\left(\frac{\varepsilon_1 {r_w}^{1-n_1}}{4}{\eta_w}^2\right) r^{1-\mathrm{n}_1}}{(2\pi)^{n_1} {h_w}^{n_1-1} b K_1}, \tag{A23}$$

$$F_2 = \frac{Q\exp\left(\frac{\varepsilon_1 {r_w}^{1-n_1}}{4n_1}{\eta_w}^2\right)}{4\pi {h_w}^{\frac{n_1-1}{n_1}} b^{\frac{1}{n_1}} K_2 \exp\left(-\frac{\varepsilon_2}{4}{\eta_R}^2\right)} \exp\left(-\frac{\varepsilon_1 \mathrm{R}^{1-\mathrm{n}_1}}{4n_1}{\eta_R}^2\right), \tag{A24}$$

$$v = \frac{\varepsilon_2}{4}\eta^2, \tag{A25}$$

$$v_R = \frac{\varepsilon_2}{4}{\eta_R}^2, \tag{A26}$$

$$W(x) = \int_x^{\infty} \frac{e^{-y}}{y} dy, \tag{A27}$$

where x can represent any real number.

References

1. Markle, J.M.; Rowe, R.K.; Novakowski, K.S. A model for the constant-head pumping test conducted in vertically fractured media. *Int. J. Numer. Anal. Methods Geomech.* **1995**, *19*, 457–473. [CrossRef]
2. Chen, Y.J.; Yeh, H.D.; Yang, S.Y. Analytical Solutions for Constant-Flux and Constant-Head Tests at a Finite-Diameter Well in a Wedge-Shaped Aquifer. *J. Hydraul. Eng.* **2009**, *135*, 333–337. [CrossRef]
3. Chen, C.C.; Chang, C.C. Well hydraulics theory and data analysis of the constant head test in an unconfined aquifer with the skin effect. *Water Resour. Res.* **2003**, *39*, 1121–1135. [CrossRef]
4. Hiller, C.K.; Levy, B.S. Estimation of aquifer diffusivity from analysis of constant-head pumping test data. *Groundwater* **1994**, *32*, 47–52. [CrossRef]
5. Lin, Y.; Li, M.; Yeh, H. An analytical model for flow induced by a constant-head pumping in a leaky unconfined aquifer system with considering unsaturated flow. *Adv. Water Resour.* **2017**, *107*, 525–534. [CrossRef]
6. Jacob, C.E. *Flow of Groundwater*; John Wiley and Sons: Hoboken, NJ, USA, 1950; pp. 321–386.
7. Chang, Y.C.; Yeh, H.D.; Chen, G.Y. Transient solution for radial two-zone flow in unconfined aquifers under constant-head tests. *Hydrol. Process.* **2010**, *24*, 1496–1503. [CrossRef]
8. Dan, H.C.; He, L.H.; Xu, B. Experimental investigation on non-Darcian flow in unbound graded aggregate material of highway pavement. *Transp. Porous Media* **2016**, *112*, 189–206. [CrossRef]
9. Jacob, C.E.; Lohman, S.W. Nonsteady flow to a well of constant drawdown in an extensive aquifer. *Eos Trans. Am. Geophys. Union* **1952**, *33*, 559. [CrossRef]
10. Liu, Z.; Xia, Y.; Shi, M.; Zhang, J. Numerical simulation and experiment study on the characteristics of non-Darcian flow and rheological consolidation of saturated clay. *Water* **2019**, *11*, 1385. [CrossRef]
11. Zhuang, C.; Zhou, Z.; Zhan, H.; Wang, J.; Li, Y.; Dou, Z. New graphical methods for estimating aquifer hydraulic parameters using pumping tests with exponentially decreasing rates. *Hydrol. Process.* **2019**, *33*, 2314–2322. [CrossRef]
12. Li, Y.; Zhou, Z.; Zhuang, C.; Huang, Y.; Wang, J. Non-Darcian effect on a variable-rate pumping test in a confined aquifer. *Hydrogeol. J.* **2020**, *28*, 2853–2863. [CrossRef]
13. Singh, S.K. Semianalytical Model for Drawdown due to Pumping a Partially Penetrating Large Diameter Well. *J. Irrig. Drain. Eng.* **2007**, *133*, 155–161. [CrossRef]
14. Yeh, H.D.; Chang, Y.C. Recent advances in modeling of well hydraulics. *Adv. Water Resour.* **2013**, *5*, 27–51. [CrossRef]
15. Xiao, L.; Ye, M.; Xu, Y.X.; Gan, F.W. A simplified solution using Izbash's equation for non-Darcian flow in a constant rate pumping test. *Ground Water* **2019**, *57*, 962–968. [CrossRef]
16. Quinn, P.M.; Parker, B.L.; Cherry, J.A. Validation of non-Darcian flow effects in slug tests conducted in fractured rock boreholes. *J. Hydrol.* **2013**, *486*, 505–518. [CrossRef]
17. Li, J.; Xia, X.H.; Zhan, H.; Li, M.; Chen, J. Non-Darcian flow for an artificial recharge well in a confined aquifer with clogging-related permeability reduction. *Adv. Water Resour.* **2021**, *147*, 103820. [CrossRef]
18. Ali, R.; Mcfarlane, D.; Varma, S.; Dawes, W.; Emelyanova, I.; Hodgson, G. Potential climate change impacts on the water balance of regional unconfined aquifer systems in south-western Australia. *J. Hydrol.* **2012**, *475*, 456–472. [CrossRef]
19. Glover, R.E.; Bittinger, M.W. Drawdown Due to Pumping From an Unconfined Aquifer. *J. Irrig. Drain. Div.* **1960**, *86*, 63–70. [CrossRef]
20. Narasimhan, T.N.; Zhu, M. Transient flow of water to a well in an unconfined aquifer: Applicability of some conceptual models. *Water Resour. Res.* **1993**, *29*, 179–192. [CrossRef]
21. Boulton, N.S. Analysis of data from non-equilibrium pumping tests allowing for delayed yield from storage. *Ice Proc.* **2015**, *26*, 469–482. [CrossRef]
22. Dupuit, J. *Etudes Théoriques et Pratiques sur le Mouvement des eaux dans les Canaux Découverts et a Travers les Terrains Permeablesm*, 2nd ed.; Hachette Livre-BNF: Maurepas, France, 1863.
23. Kruseman, G.P.; Ridder, N.A.D.; Verweij, J.M. *Analysis and Evaluation of Pumping Test Data*, 2nd ed.; International Institute for Land Reclamation and Improvement: Wageningen, The Netherlands, 1991.
24. Bresciani, E.; Davy, P.; De Dreuzy, J.R. Is the Dupuit assumption suitable for predicting the groundwater seepage area in hillslopes? *Water Resour. Res.* **2014**, *50*, 2394–2406. [CrossRef]
25. Dagan, G. A method of determining the permeability and effective porosity of unconfined anisotropic aquifers. *Water Resour. Res.* **1967**, *3*, 1059. [CrossRef]
26. Neuman, S.P. Analysis of pumping test data from anisotropic unconfined aquifers considering delayed gravity response. *Water Resour. Res.* **1975**, *11*, 329–342. [CrossRef]
27. Pistiner, A. Unconfined aquifer flow theory-from Dupuit to present. *Open J. Fluid Dyn.* **2015**, *5*, 51–57. [CrossRef]
28. Wen, Z.; Huang, G.; Zhan, H.; Li, J. Two-region non-Darcian flow toward a well in a confined aquifer. *Adv. Water Resour.* **2008**, *31*, 818–827. [CrossRef]
29. Li, Y.; Zhou, Z.; Shen, Q.; Zhuang, C.; Wang, P. Two-region Darcian and non-Darcian flow towards a well with exponentially decayed rates considering time-dependent critical radius. *J. Hydrol.* **2021**, *601*, 126712. [CrossRef]
30. Ya-Chi, C.; Hund-Der, Y. Skin effect in generalized radial flow model in fractured media. *Geophys. J. Int.* **2011**, *185*, 78–84.
31. Malama, B.; Kuhlman, K.L.; Revil, A. Theory of transient streaming potentials associated with axial-symmetric flow in unconfined aquifers. *Geophys. J. Int.* **2009**, *179*, 990–1003. [CrossRef]

32. Mathias, S.A.; Butler, A.P.; Zhan, H.B. Approximate solutions for Forchheimer flow to a well. *J. Hydraul. Eng.* **2008**, *134*, 1318–1325. [CrossRef]
33. Sen, Z. Non-Darcian groundwater flow in leaky aquifers. *Hydrol. Sci. J.* **2000**, *45*, 595–606. [CrossRef]
34. Wen, Z.; Huang, G.H.; Zhan, H.B. An analytical solution for non-Darcian flow in a confined aquifer using the power law function. *Adv. Water Resour.* **2008**, *31*, 44–55. [CrossRef]
35. Wen, Z.; Huang, G.H.; Zhan, H.B. Non-Darcian flow to a well in an aquifer–aquitard system. *Adv. Water Resour.* **2008**, *31*, 1754–1763. [CrossRef]
36. Moench, A.F.; Prickett, T.A. Radial flow in an infinite aquifer undergoing conversion from artesian to hydraulic head conditions. *Water Resour. Res.* **1972**, *8*, 494–499. [CrossRef]
37. Sen, Z. Nonlinear flow toward wells. *J. Hydraul. Eng.* **1989**, *115*, 193–209. [CrossRef]
38. Chui, T.; Freyberg, D.L. The use of COMSOL for integrated hydrological modeling. In Proceedings of the COMSOL Conference, Grenoble, France, 23 October 2007.
39. Jones, L.; Lemar, T.; Tsai, C.-T. Results of two pumping tests in Wisconsin age weathered till in Iowa. *Ground Water* **1992**, *30*, 529–538. [CrossRef]